



# HHS Public Access

Author manuscript

*Mol Psychiatry*. Author manuscript; available in PMC 2016 October 20.

Published in final edited form as:

*Mol Psychiatry*. 2016 November ; 21(11): 1517–1526. doi:10.1038/mp.2015.219.

## **KCNH2-3.1 expression impairs cognition and alters neuronal function in a model of molecular pathology associated with schizophrenia**

Gregory V. Carr<sup>#1</sup>, Jingshan Chen<sup>#2</sup>, Feng Yang<sup>1</sup>, Ming Ren<sup>1</sup>, Peixiong Yuan<sup>1</sup>, Qingjun Tian<sup>1</sup>, Audrey Bebensee<sup>2</sup>, Grace Y. Zhang<sup>2</sup>, Jing Du<sup>2</sup>, Paul Glineburg<sup>2</sup>, Randy Xun<sup>1,2</sup>, Omoye Akhile<sup>2</sup>, Daniel Akuma<sup>1</sup>, James Pickel<sup>3</sup>, James C. Barrow<sup>1,4</sup>, Francesco Papaleo<sup>5</sup>, and Daniel R. Weinberger<sup>1,6,\*</sup>

<sup>1</sup>Lieber Institute for Brain Development, Johns Hopkins University Medical Campus, Baltimore, MD, 21205, USA

<sup>2</sup>Clinical Brain Disorders Branch; Genes, Cognition and Psychosis Program, National Institute of Mental Health, Bethesda, MD, 20814, USA

<sup>3</sup>Transgenic Core Facility, National Institute of Mental Health, Bethesda, MD, USA

<sup>4</sup>Department of Pharmacology and Molecular Sciences, Johns Hopkins School of Medicine, Baltimore, Maryland, 21205, USA

<sup>5</sup>Department of Neuroscience and Brain Technologies, Istituto Italiano di Tecnologia, via Morego, 30, 16163 Genova, Italy

<sup>6</sup>Departments of Psychiatry, Neurology, Neuroscience and The McKusick-Nathan Institute of Genetic Medicine, Johns Hopkins School of Medicine, Baltimore, Maryland, 21205, USA

# These authors contributed equally to this work.

### **Abstract**

Overexpression in humans of *KCNH2-3.1*, which encodes a primate-specific and brain-selective isoform of the human ether-a-go-go-related (hERG) potassium channel, is associated with impaired cognition, inefficient neural processing, and schizophrenia. Here, we describe a new mouse model that incorporates the *KCNH2-3.1* molecular phenotype. *KCNH2-3.1* transgenic mice are viable and display normal sensorimotor behaviors. However, they show alterations in neuronal structure and microcircuit function in the hippocampus and prefrontal cortex, areas affected in schizophrenia. Specifically, in slice preparations from the CA1 region of the hippocampus, *KCNH2-3.1* transgenic mice have fewer mature dendrites and impaired theta burst stimulation long-term potentiation (TBS-LTP). Abnormal neuronal firing patterns characteristic of the fast deactivation kinetics of the *KCNH2-3.1* isoform were also observed in prefrontal cortex.

Users may view, print, copy, and download text and data-mine the content in such documents, for the purposes of academic research, subject always to the full Conditions of use:[http://www.nature.com/authors/editorial\\_policies/license.html#terms](http://www.nature.com/authors/editorial_policies/license.html#terms)

\*Correspondence should be addressed to: Gregory V. Carr and Daniel R. Weinberger, Lieber Institute for Brain Development, 855 North Wolfe Street, Baltimore, MD 21205, 410-955-1000, greg.carr@libd.org, drweinberger@libd.org.

**Conflicts of Interest** Dr. Weinberger is an inventor on an NIH- held patent “Schizophrenia related isoform of KCNH2 and development of antipsychotic drugs” (US patent No. 8101380).

Transgenic mice showed significant deficits in a hippocampal-dependent object location task and a prefrontal cortex-dependent T-maze working memory task. Interestingly, the hippocampal-dependent alterations were not present in juvenile transgenic mice, suggesting a developmental trajectory to the phenotype. Suppressing *KCNH2-3.1* expression in adult mice rescues both the behavioral and physiological phenotypes. These data provide insight into the mechanism of association of *KCNH2-3.1* with variation in human cognition and neuronal physiology and may explain its role in schizophrenia.

## Keywords

cognition; schizophrenia; *KCNH2*; learning and memory; hippocampus; prefrontal cortex

---

## Introduction

Polymorphisms in the *KCNH2* gene have been associated with altered cognitive function and with schizophrenia in several independent clinical data sets (1–3). The *KCNH2* gene encodes the human ether-a-go-go related (hERG) voltage-gated potassium channel (4, 5). The risk-associated alleles predict impaired cognitive function in both patients and healthy controls as well as overexpression in brain of *KCNH2-3.1*, a truncated isoform with unique electrophysiological properties(1). *KCNH2-3.1* is a primate-specific isoform, enriched in the brain, which lacks the Per-Arnt-Sim (PAS) domain critical for the slow-deactivation properties of hERG channels. Rat cortical neurons expressing *KCNH2-3.1*-containing ERG channels have higher firing rates and faster ERG channel deactivation kinetics(1). In general, ERG channels have been shown to regulate the activity of neurons in multiple brain regions (6, 7). Thus, these findings suggest that a possible cause of the cognitive dysfunction in patients with schizophrenia associated with elevated *KCNH2-3.1* may be decreased synchrony among functionally connected neurons(8). Indeed, people who carry alleles associated with higher expression of *KCNH2-3.1* exhibit more inefficient neuronal processing in the hippocampus and frontal cortex during memory tasks as measured with fMRI(1).

Cognitive dysfunction associated with schizophrenia is a major unmet therapeutic need, with important implications for functional outcomes in patients (9, 10). Many risk factors associated with impaired cognition in schizophrenia have been identified, including genes and environmental factors, but their potential role in the development of new therapies has been the subject of few investigations (11, 12). The identification of novel treatments for schizophrenia, either designed to remediate or prevent the symptoms, will require greater insight into the functional role of these risk factors in the underlying psychopathology of the disorder. Recent investigations of *KCNH2* in relation to schizophrenia have shown that the genotype associated with increased expression of the *KCNH2-3.1* isoform predicts enhanced response to antipsychotic drug therapy, suggesting that targeted modulation of 3.1 hERG channel isoform activity may be a viable drug discovery strategy (7, 13)

In the following experiments, we describe the characterization of a transgenic mouse model of the molecular phenotype associated with increased expression of the *KCNH2-3.1*

isoform. This new transgenic mouse incorporates a potential molecular risk factor for cognitive disturbance associated with schizophrenia; thus, it may contribute to a deeper understanding of the neurobiological bases of schizophrenia-relevant deficits and be of value in the development of novel therapies. Specifically, these mice exhibit deficits in hippocampal- and prefrontal-cortex mediated cognition and altered neural processing analogous to deficits seen in people that overexpress the *KCNH2-3.1* isoform.

## Materials and Methods

### KCNH2-3.1 isoform cloning

KCNH2-3.1 cDNA was generated with the 5'-RACE system (Invitrogen, Carlsbad, CA) by long PCR with specific primers and high-fidelity DNA polymerase, cloned into a pZero-Blunt vector, and then subcloned into pcDNA3.1 (Invitrogen).

### KCNH2-3.1 transgenic mice

All of the mice were maintained in strict accordance with National Institutes of Health animal care guidelines and the procedures described were approved by the NIMH and SoBran Biosciences, Inc. Animal Care and Use Committees. To develop the mice, *KCNH2-3.1* cDNA was subcloned from pcDNA3.1 into a pTet-splice to generate an inducible pTetOp-*KCNH2-3.1* vector. The pTetOp-*KCNH2-3.1* DNA was microinjected into the pro-nuclei of the oocytes from SJL × C57BL6 mice to generate transgenic mouse lines. Tail DNA samples from resulting mice were isolated and genotyped for the transgene by PCR. These mice were crossbred with mice expressing the tetracycline transactivator (tTA) gene under the control of the neuron-specific enolase (NSE) promoter (NSE-tTA mice; C57BL/6 background) to produce conditional transgenic mice (Figure 1a). The transgenic mice were backcrossed with C57BL/6 mice (5 generations). The *KCNH2-3.1*-NSE-tTA+ sibling mice were used as controls. Male mice between PD56-PD180 (~2–6 months of age) were used for all testing except for the electrophysiological and behavioral studies in juvenile (PD16–22) mice. In this article, all mice called “KCNH2-3.1 transgenic mice” were heterozygous for the *KCNH2-3.1* transgene and either heterozygous or homozygous for the NSE-tTA transgene due to breeding double transgenic males (hemizygous for both transgenes) and NSE-tTA (hemizygous) females. Additionally, all mice referred to as “control” are NSE-tTA transgenic littermates (hemizygous or homozygous). The performance of NSE-tTA transgenic mice in the object location task was compared to wild-type C57BL/6J mice purchased from The Jackson Laboratory. A second, independent line of *KCNH2-3.1* transgenic mice were also tested in the object location task in order to verify the behavioral effects caused by expression of the transgene. All mice, except those used in the T-maze experiment, were group-housed (2–4/cage). All mice were housed in a climate-controlled animal facility (22±2°C) and maintained on a 12-hr light/dark cycle with lights on at 0600 hours.

### RNA extraction and qRT-PCR

Total RNA was isolated from homogenized tissue using RNeasy Lipid Tissue Mini Kit (Qiagen, Valencia CA. Cat# 74804). qRT-PCR was performed using Applied Biosystems' TaqMan gene expression assay kits per the manufacturer's instructions (Applied Biosystems/Life Technologies, Carlsbad, CA). In brief, total RNA was reverse-transcribed with the high

capacity cDNA reverse transcription kit (Applied Biosystems, Cat# 4368814) on GeneAmp 9700 thermal cycler. The RT product (cDNA) then entered a 40-cycle real time PCR with the corresponding PCR primers (5'-ATGTCCTCCCACTCTGCAGGGA-3' and 5'-GAAGGTCTTGCGCGGCCTG-3') on an Applied Biosystems 7900HT Fast Real-Time PCR System. Mouse beta-actin (ACTB, Cat# 4352341E) was used as reference gene.

## Electrophysiological methods

**Hippocampal Field Recording**—Coronal hippocampal slices (400  $\mu\text{m}$ ) were prepared in accordance with NIH guidelines. Briefly, hippocampal slices were cut using a vibrating blade microtome (Leica VT1000S, Leica Systems) in ice-cold slicing buffer (in mM: 250 sucrose, 2.5 KCl, 1.25  $\text{NaH}_2\text{PO}_4$ , 26  $\text{NaHCO}_3$ , 0.5  $\text{CaCl}_2$ , 4.0  $\text{MgCl}_2$ , and 10 D-Glucose) bubbled with 95%  $\text{O}_2$  and 5%  $\text{CO}_2$ . Slices were then transferred to a holding chamber containing oxygenated artificial cerebrospinal fluid (aCSF; in mM: 125 NaCl, 2.5 KCl, 1.25  $\text{NaH}_2\text{PO}_4$ , 2  $\text{CaCl}_2$ , 1  $\text{MgCl}_2$ , 26  $\text{NaHCO}_3$  and 10 glucose) for 30 min at 34°C and for another 30 min at 22°C for recovery, and then transferred to a submersion recording chamber continually perfused with 32°C oxygenated aCSF (rate: 2 ml/min). Slices were equilibrated for at least 15 min before each recording. aCSF-filled glass electrodes (resistance <1 M $\Omega$ ) were positioned in the stratum radiatum of area CA1 for extracellular recording. Synaptic responses were evoked by stimulating Schaffer collaterals with 0.1 ms pulses with a bipolar tungsten electrode (WPI Inc., Sarasota, FL) once every 20 s. The stimulation intensity was systematically increased to determine the maximal field excitatory post-synaptic potential (fEPSP) slope and then adjusted to yield 40–60% of the maximal (fEPSP) slope. Experiments with maximal fEPSPs of less than 0.15 mV or with substantial changes in the fiber volley were rejected. After recording of a stable baseline for at least 15 min, TBS-LTP was induced by 4 TBS events (4 bursts, each of 4 pulses at 100 Hz); HFS-LTP was induced by 4 trains of high frequency stimulation (4 trains, 100 Hz, 100 pulses, 20 s train interval). Field EPSPs were recorded (Axopatch 200B amplifier, Molecular Devices, Sunnyvale, CA), filtered at 2 kHz, digitized at 10 kHz (Axon Digidata 1321A), and stored for off-line analysis (Clampfit 10). Initial slopes of fEPSPs were expressed as percentages of baseline averages. In summary graphs, each point represents the average of 3 consecutive responses. The time-matched, normalized data were averaged across experiments and expressed as means $\pm$ SEM.

**Medial Prefrontal Whole-Cell Recording**—Control NSE-tTA (*KCNH2*<sup>-/+</sup>) and *KCNH2*-3.1 transgenic (*KCNH2*<sup>+/+</sup>) mice at ages of postnatal days of 50–72 were used in this study. The brains were quickly removed after isoflurane anesthesia, and 300- $\mu\text{m}$  thick coronal slices containing frontal cortex were cut on a vibrating microtome (VF-200 Microtome, Precisionary Instruments, Greenville, NC). The slice cuttings were maintained in oxygenated ice-cold  $\text{Na}^+$ -free sucrose solution containing (in mM) 2.5 KCl, 1.25  $\text{NaH}_2\text{PO}_4$ , 26  $\text{NaHCO}_3$ , 0.5  $\text{CaCl}_2$ , 4.0  $\text{MgCl}_2$ , 10 glucose and 250 sucrose bubbled with 95%  $\text{O}_2$  and 5%  $\text{CO}_2$ . The slices were initially incubated at 35°C in Ringer solution (aCSF bubbled with 95%  $\text{O}_2$  and 5%  $\text{CO}_2$ ) containing (in mM) 124 NaCl, 2.5 KCl, 1.25  $\text{NaH}_2\text{PO}_4$ , 2  $\text{CaCl}_2$ , 1  $\text{MgSO}_4$ , 26  $\text{NaHCO}_3$  and 10 glucose, pH 7.4, and then kept at room temperature. The slices were transferred into a recording chamber at approximately 32–34°C. For current clamp and voltage clamp, the recording pipettes were filled with intracellular solution

containing (in mM) 120 K-gluconate, 6 KCl, 0.5 CaCl<sub>2</sub>, 0.2 EGTA, 4 ATP-Mg, 10 HEPES, and 0.3% biocytin, with a final pH of 7.25. The resistances of patch pipettes were 3–6 M $\Omega$ . After whole-cell configuration was achieved, series resistance were compensated by 80–90% and monitored periodically. Most pyramidal neurons at deep layers of frontal cortex had series resistance around 7–8 M $\Omega$  (range, 4–13 M $\Omega$ ). A small percentage of pyramidal neurons with a resting membrane potential less than –50 mV, or gradual changes in membrane potential, input resistance or action potential amplitudes, were considered as unhealthy and discarded. For current-clamp recordings, a depolarizing current step was injected to induce multiple action potentials in the pyramidal neurons, and action potential numbers were plotted against the depolarizing currents injected into the pyramidal neurons. For voltage-clamp recordings, voltage protocols given by pClamp 10 (Molecular Devices, CA) were delivered to the pyramidal neurons through the patch pipette in the presence of 1.5  $\mu$ M tetrodotoxin (Sigma) to block voltage-gated sodium currents. E-4031-sensitive tail currents including *KCNH2-1A* and *KCNH2-3.1*-mediated tail currents were generated by subtracting the before inhibitor and after inhibitor currents. The decay of *KCNH2* currents in the pyramidal neurons, attributed to channel deactivation, was fitted by single- or double-exponential functions. The signals were amplified and filtered at 2 kHz with Axopatch 200B and acquired at sampling intervals of 20–100  $\mu$ s through a DigiData 1321A interface with program pCLAMP 10. The data was evaluated with paired t-tests and presented as mean  $\pm$  standard error.

### Behavioral testing

**Object location**—The object location test was modified from a previously published protocol(14). The testing apparatus was an acrylic open field arena (42  $\times$  42  $\times$  30 cm). On day 1 of testing, mice were allowed to freely explore the empty arena for 60 minutes under red light settings (8  $\pm$  2 lux). On day 2, mice were placed back into the open field for a 10 min period where they were allowed to explore two identical copies of an object. The objects were either rectangular boxes (4  $\times$  4  $\times$  7 cm) or Erlenmeyer flasks (4  $\times$  7 cm). Both types of objects could be either white or black. One hour later, mice were returned to the arena for the test phase and allowed to explore one copy of the object in the same location as during the sample phase and one copy of the object in a novel location. The two sessions were videotaped and the total exploration time was recorded. The discrimination ratio in the test phase was calculated as the amount of time spent exploring the object in the familiar location subtracted from the time exploring the object in the displaced location divided by the total exploration time. The videotapes were scored by a trained observer blind to genotype and treatment. A pre-established exclusion criterion was set so that mice had to explore objects for at least 4 seconds during each phase of the test in order to be included in the study. Three control mice and four *KCNH2-3.1* transgenic mice failed to reach exploration time criterion.

### Drug treatment

In order to turn off expression of the *KCNH2-3.1* transgene, *KCNH2-3.1* transgenic and control mice were treated with doxycycline hyclate (200  $\mu$ g/mL; Sigma-Aldrich, St. Louis, MO, USA) in their drinking water or food (625 mg/kg of diet; Harlan, Indianapolis, IN,

USA) for a minimum of three weeks. Opaque water bottles were used and the water was changed every three days. Doxycycline-treated food was changed weekly.

### Statistical analyses

Data are represented throughout as the mean  $\pm$  SEM and individual data points are biological replicates. Two sided T-tests and ANOVAs were used to analyze the data for the *KCNH2-3.1* expression, object location, and electrophysiological experiments. Significance was set at a  $p$ -value  $< 0.05$ . Bonferroni's post hoc tests were used to determine differences between groups following ANOVAs. All data sets met the assumptions (e.g. normal distribution, etc.) of the statistical test used. No statistical methods were used to estimate sample size and no randomization procedure was used for group assignment.

## Results

### *KCNH2-3.1* inducible expression in transgenic mice

Figure 1a is a schematic of the construct used to produce the *KCNH2-3.1* transgenic mice. This construct facilitates conditional expression of the *KCNH2-3.1* transgene under the control of the neuron-specific enolase promoter. Expression of the *KCNH2-3.1* transgene can be regulated by tetracycline antibiotics, including doxycycline (“tet-off” system). We confirmed expression of *KCNH2-3.1* mRNA in prefrontal cortex tissue of the double transgenic mice with RT-qPCR (Figure 1b). The control lanes show no *KCNH2-3.1* mRNA in samples from mice that did not have both the *KCNH2-3.1* and NSE-tTA transgenes, demonstrating that there was no endogenous *KCNH2-3.1* expression or “leaky” *KCNH2-3.1* transgene expression in the absence of the NSE-tTA promoter. In the *KCNH2-3.1* lanes, genomic DNA contamination was not present, as there was no expression in the samples run without reverse transcriptase (RT-). The samples from mice expressing both transgenes run with reverse transcriptase (RT+) show a clear band corresponding to *KCNH2-3.1* cDNA. Mouse  $\beta$ -actin was measured as a control. *KCNH2-3.1* mRNA was present in the four brain regions sampled (cerebellum, prefrontal cortex, hippocampus, and striatum) (Figure 1c). We also tested whether chronic treatment with doxycycline could alter expression of the *KCNH2-3.1* transgene (Figure 1d). We measured *KCNH2-3.1* expression in homogenized prefrontal cortex tissue from mice treated with doxycycline for three weeks. As expected, control mice, those having only the NSE-tTA transgene, did not express the *KCNH2-3.1* transgene. Doxycycline treatment produced a roughly 80% reduction in *KCNH2-3.1* expression (Figure 1d). These data demonstrate the viability and controllability of the *KCNH2-3.1* expression system employed in these experiments.

### *KCNH2-3.1* mice are viable, display no differences in locomotor activity, sensorimotor behavior, or fear conditioning compared to control mice

General health, as previously described (15), was tested in adult mice. *KCNH2-3.1* transgenic mice did not differ on measures of physical condition, motor reflexes, or home cage behavior (Supplementary Table 1). There were no differences in baseline open-field locomotor activity (Supplementary Figure 1). Sensorimotor gating, measured using the prepulse inhibition (PPI) test (Supplementary Figure 2), and fear conditioning (cued and contextual; Supplementary Figure 3) were normal in *KCNH2-3.1* transgenic mice. These

data suggest that general physical and basic cognitive processes are intact in *KCNH2-3.1* transgenic mice.

### **KCNH2-3.1 transgenic mice show impaired TBS-induced LTP and neuronal activity in the CA1 region of the hippocampus**

Humans with *KCNH2* genotypes associated with increased brain levels of *KCNH2-3.1* exhibit inefficient neural processing in the hippocampus (1). In order to test potentially analogous processes in the *KCNH2-3.1* transgenic mice, we first measured neuronal activity in pyramidal cells in the CA1 region in slice preparations. Hippocampal slices from *KCNH2-3.1* transgenic mice demonstrated impaired LTP amplitude compared to control mice. Figure 2a compares fEPSP recordings before LTP induction (black lines) and 60 minutes after LTP induction (red lines). The fEPSP amplitude was significantly lower in the *KCNH2-3.1* transgenic mice. The complete time course following LTP induction showed that the difference at 60 minutes was due to rapid decay of the induction effect (Figure 2b). The LTP deficit appears to be due to postsynaptic mechanisms because paired pulse facilitation is normal and field EPSP magnitude is significantly lower in *KCNH2-3.1* transgenic mice across multiple stimulus intensities (Figure 2c and 2d). These results indicate that *KCNH2-3.1* transgenic mice have impaired hippocampal synaptic plasticity that may affect CA1-dependent information processing.

### **KCNH2-3.1 expression is associated with decreased dendritic spine density in the CA1 region of the hippocampus**

One potential substrate for the electrophysiological deficits in the *KCNH2-3.1* transgenic mice could be alterations in synapse structure. Analyses of dendritic spines in CA1 of adult mice showed that *KCNH2-3.1* transgenic mice have significantly fewer mushroom-shaped and stubby spines with no change in the number of filopodia (Supplementary Figure 4). These data suggest a decrease in mature synapses in adult *KCNH2-3.1* transgenic mice compared to their littermate controls.

### **KCNH2-3.1 transgenic mice have impaired hippocampal-dependent memory**

Based on their abnormal hippocampal morphology and neuronal activity, we next investigated hippocampal-dependent cognitive function in *KCNH2-3.1* transgenic mice. The object location task is a one-trial learning paradigm in which mice recognize a change in the orientation of objects within a familiar environment. Mice generally spend more time exploring displaced objects as a measure of recognition memory. The object location task is specifically dependent on intact hippocampal function(16). Studies comparing the control littermates to wild-type C57BL/6J mice showed normal object location performance in the control mice (Supplementary Figure 5a). There was no difference in the amount of time *KCNH2-3.1* transgenic mice spent exploring the displaced object compared to the object in the familiar location, indicating a complete lack of recognition in this task. The apparent recognition deficit was not due to any change in total exploration as the difference in exploration time between *KCNH2-3.1* transgenic mice and their littermate controls was not significant (Figure 3b). In order to confirm that the object location deficit was due to *KCNH2-3.1* expression and not non-specific effects due to the location of transgene insertion, we tested a second, independent line of *KCNH2-3.1* mice in the object location

task. This second *KCNH2-3.1* line also exhibited significant impairment in object location recognition (Supplementary Figure 5c).

Interestingly, this object location deficit did not generalize to other object recognition tasks. *KCNH2-3.1* mice showed normal recognition in the novel object recognition task and the temporal order object recognition task. (Supplementary Figure 6 and 7)(14, 16). Moreover, the deficit in the object location task did not generalize to other hippocampal-dependent memory tasks. *KCNH2-3.1* transgenic mice performed normally in the Barnes maze and showed normal trace fear conditioning (Supplementary Figures 8 and 9), suggesting the cognitive deficits exhibited by *KCNH2-3.1* transgenic mice are not representative of global hippocampal dysfunction, but are context dependent. Further, the ongoing effects of *KCNH2-3.1* expression during adulthood appeared to underlie the object location and LTP deficits as treatment with doxycycline reversed both phenotypes in *KCNH2-3.1* transgenic mice without affecting the performance of control mice (Figure 3c–d).

### ***KCNH2-3.1* expression alters neuronal firing in the PFC**

Humans with genetically predicted increases in brain expression of *KCNH2-3.1* in the hippocampus also had increases in the ratio of *KCNH2-3.1* to the full-length isoform in the PFC, suggesting potential disruption of the heterodimer composition of hERG channels in the region(17). The modified expression pattern was associated with inefficient processing within the PFC during the N-back working memory task measured with fMRI. Additionally, transfection of *KCNH2-3.1* into rat cortical neurons resulted in an increase in the firing rate and faster ERG channel deactivation kinetics than found in neurons only expressing the full-length isoform(1). We found a remarkably similar phenotype in PFC slices taken from the *KCNH2-3.1* transgenic mice. In Figure 4a, we identified a current sensitive to attenuation by the ERG channel blocker E-4031 in both *KCNH2-3.1* transgenic mice and their littermate controls. *KCNH2-3.1* transgenic mice show lower values for both the  $\tau_1$  (lower) and  $\tau_2$  (upper) deactivation constants indicative of the relatively fast deactivation properties of the *KCNH2-3.1* isoform (Figure 4b). Faster deactivation in the *KCNH2-3.1* transgenic mice translated into an increase in the firing rate for neurons in the PFC, a finding also strikingly similar to that reported previously in primary cortical neuron culture experiments (Figure 4c and d)(1). The changes in neuronal activity caused by *KCNH2-3.1* expression within the PFC could underlie functional modifications in PFC-dependent behavior.

### ***KCNH2-3.1* mice exhibit impaired spatial working memory in a PFC-dependent T-maze task**

We next tested *KCNH2-3.1* transgenic mice in the discrete paired-trial variable-delay T-maze task. This version of the T-maze requires intact signaling within the PFC for normal performance (18, 19). *KCNH2-3.1* transgenic mice were able to learn the non-match to sample rule in the same number of training sessions as the control mice (Supplementary Figure 10a). Moreover, there was no difference in the number of mice that reached criterion before the 20-day cutoff as two mice from each genotype failed to reach the accuracy threshold during training. During the variable intra-trial delay portion of the task, both genotypes showed a significant decrease in performance as the delay period increased (Supplementary Figure 10b). However, there was a significant difference between genotypes on 4-s delay trials as *KCNH2-3.1* transgenic mice were less accurate compared to control

mice. These data suggest impaired working memory at a delay interval thought to be dependent on intact prefrontal cortex function (15, 19, 20).

### **Hippocampal-dependent functional deficits in adult *KCNH2-3.1* transgenic mice are not present in juveniles**

Because the diagnostic symptoms of schizophrenia generally present during early adulthood, it has been hypothesized that early developmental antecedents may interact with developmental changes in the brain later in life to precipitate the emergence of the illness phenotype (21). We thus decided to investigate the functional consequences of *KCNH2-3.1* expression during the prepubertal juvenile stage of development. Figure 5a shows representative control and *KCNH2-3.1* transgenic mouse recording traces taken from the CA1 region of the hippocampus with strikingly similar profiles. In contrast to their adult counterparts, *KCNH2-3.1* transgenic mice showed no difference compared to littermate controls on measures of TBS-LTP or fEPSP amplitude (Figure 5b and c). In agreement with the adult data, there was no difference in paired-pulse facilitation (Figure 5d). These data indicate that the LTP alterations seen in adult *KCNH2-3.1* transgenic mice are emergent phenomena that develop later in neural development.

We next investigated if there were any behavioral differences between juvenile and adult *KCNH2-3.1* transgenic mice that correlated with the effects in CA1 function. In the object location test, where adult transgenic mice had significant deficits in recognizing the displaced object, juvenile transgenic mice showed no differences compared to their control littermates (Figure 5e).

## **Discussion**

Animal models of genetic risk for the cognitive deficits associated with schizophrenia can serve as valuable platforms for studying the pathophysiology and potential treatment of the disorder(22). Here we report the characterization and functional validation of a mouse model of increased expression of the *KCNH2-3.1* isoform of the hERG channel and cognitive dysfunction. Polymorphisms in the *KCNH2* gene associated with increased expression of the *KCNH2-3.1* isoform in humans are related to altered cognitive function and cortical physiology in patients with schizophrenia(1). We created transgenic mice that express the *KCNH2-3.1* isoform in brain and describe physiological, structural, and cognitive characteristics that instantiate these mice as a model system for exploring aspects of the molecular biology of cognitive dysfunction associated with schizophrenia.

The hippocampus shows significant molecular and functional alterations in patients with schizophrenia (reviewed in (23, 24)). Specifically, post-mortem analysis and imaging studies find that hippocampal volume is decreased in patients with schizophrenia(25–27), who also are impaired in hippocampal-dependent tasks(28, 29). *KCNH2-3.1* transgenic mice show some analogous morphological and functional features. Decreased spine density and formation of mushroom spines implicate a structural component to the physiological and behavioral associations seen in these mice (30). Interestingly, the behavioral deficits in hippocampal-dependent tasks seen in the *KCNH2-3.1* transgenic mice were fairly selective. The mice were only impaired in the object location task while performance was largely

intact in the Barnes maze, temporal order object recognition, contextual fear conditioning, and trace fear conditioning. Additionally, performance was normal in the novel object recognition task, which is dependent on the perirhinal cortex, a perihippocampal structure (14, 31, 32). The general lack of impairment in hippocampal-dependent tasks was surprising given the abnormal firing activity and impaired TBS-LTP within CA1, a region implicated in these behaviors (33, 34). Our behavioral findings suggest that meaningful information processing still occurs in the CA1 region of *KCNH2-3.1* transgenic mice despite an almost complete lack of TBS-LTP. This is in line with previous data showing that mice with similar impairments in TBS-LTP and the object location test show relatively normal performance in the Morris water maze and contextual fear conditioning (35). These data support a framework of context-dependent segregation among so-called hippocampal-dependent tasks. One hypothesis is that TBS-LTP is required for the identification of subtle differences in contextual orientation, similar to the discriminations required in the object location test, while hippocampal-dependent temporal discriminations and spatial reference memory are less perturbed by the loss of TBS-LTP.

Interestingly, juvenile *KCNH2-3.1* transgenic mice did not exhibit the alterations in hippocampal function seen in adult mice, suggesting a possible developmental trajectory to the phenotype. Analogous delayed emergence of behavioral phenotypes has been described for other developmental models associated with schizophrenia (36–39). In this context it is noteworthy that reducing expression of the *KCNH2-3.1* transgene following treatment with doxycycline reverses the deficit in the object location task and the deficit in hippocampal LTP. These findings suggest that sub-chronic or acute modulation of hERG channel function during adult life may be a viable strategy for improving the cognitive impairment associated with *KCNH2* risk factors.

Along with the hippocampus, the PFC is a region thought to be critically involved in the dysfunction present in schizophrenia (40). *KCNH2-3.1* expression produces impairments in the PFC analogous in some respects to those produced in the hippocampus. Alterations in neuronal firing in the PFC have been shown to impair multiple cognitive domains, including working memory (41–43). PFC neurons of *KCNH2-3.1* transgenic mice had a higher basal firing rate and faster hERG channel deactivation kinetics compared to their control littermates. These observations were similar to those previously described in primary neuronal culture and Chinese hamster ovary CHO cells after overexpression of *KCNH2-3.1* (1, 44). These modifications in neuronal activity have a potentially large effect on neuronal synchronization and specific oscillations that are critical for normal brain function (45–47). Our data indicate that *KCNH2-3.1* transgenic mice have slight deficits in a PFC-dependent working memory T-maze task only with a short 4-second interval delay, again suggesting selective and subtle deficits in frontal lobe functions.

Despite these apparent deficits in hippocampal and PFC functioning, the behavioral phenotype present in *KCNH2-3.1* transgenic mice appeared more subtle than would be expected in a comprehensive model of cognitive dysfunction relevant to schizophrenia (48). However, we propose that the *KCNH2-3.1* transgenic mouse is a model of genetic risk for cognitive dysfunction in schizophrenia. The intermediate behavioral profile of *KCNH2-3.1* transgenic mice is very similar to cognitive deficits in people that carry validated genetic risk

factors, but do not have the full disorder(1). Moreover, it is unclear what cognitive deficits in a mouse model would best reproduce the cognitive deficits of schizophrenia, which themselves are complex and variable.

The prevailing hypothesis concerning the etiology of schizophrenia, and many other complex psychiatric disorders, is that genetic risk factors interact with environmental risk factors relatively early in development to cause the disorder(49). It is not known which combinations of how many risk factors directly lead to schizophrenia in individual patients. *KCNH2-3.1* transgenic mice provide a potentially valuable platform for modeling environment risk factors that might interact with *KCNH2-3.1* expression in the human population and also provide information on the neurobiology specific to its role as a potential risk factor. Finally, because hERG channels are targeted by almost all currently available antipsychotic drugs, and because *KCNH2* genotype associated with increased brain expression of the 3.1 isoform predicts enhanced response to these clinical agents(13), the *KNCH2-3.1* transgenic mouse is an appealing model to test new drugs that affect the activity of this brain-enriched potassium channel.

## Supplementary Material

Refer to Web version on PubMed Central for supplementary material.

## Acknowledgments

This work was funded by the Intramural Research Program of the National Institute of Mental Health to the Weinberger Lab, US National Institute of Mental Health grant R01MH101102, and the Lieber Institute for Brain Development.

## References

- Huffaker SJ, Chen J, Nicodemus KK, Sambataro F, Yang F, Mattay V, et al. A primate-specific, brain isoform of KCNH2 affects cortical physiology, cognition, neuronal repolarization and risk of schizophrenia. *Nat Med*. 2009; 15(5):509–18. [PubMed: 19412172]
- Hashimoto R, Ohi K, Yasuda Y, Fukumoto M, Yamamori H, Kamino K, et al. The KCNH2 gene is associated with neurocognition and the risk of schizophrenia. *World J Biol Psychiatry*. 2013; 14(2): 114–20. [PubMed: 21936766]
- Atalar F, Acuner TT, Cine N, Oncu F, Yesilbursa D, Ozbek U, et al. Two four-marker haplotypes on 7q36.1 region indicate that the potassium channel gene HERG1 (KCNH2, Kv11.1) is related to schizophrenia: a case control study. *Behav Brain Funct*. 2010; 6:27. [PubMed: 20507645]
- Trudeau MC, Warmke JW, Ganetzky B, Robertson GA. HERG, a human inward rectifier in the voltage-gated potassium channel family. *Science*. 1995; 269(5220):92–5. [PubMed: 7604285]
- Trudeau MC, Warmke JW, Ganetzky B, Robertson GA. HERG sequence correction. *Science*. 1996; 272(5265):1087. [PubMed: 8638148]
- Pessia M, Servetini I, Panichi R, Guasti L, Grassi S, Arcangeli A, et al. ERG voltage-gated K<sup>+</sup> channels regulate excitability and discharge dynamics of the medial vestibular nucleus neurones. *J Physiol*. 2008; 586(Pt 20):4877–90. [PubMed: 18718985]
- Ji H, Tucker KR, Putzier I, Huertas MA, Horn JP, Canavier CC, et al. Functional characterization of ether-à-go-go-related gene potassium channels in midbrain dopamine neurons - implications for a role in depolarization block. *Eur J Neurosci*. 2012; 36(7):2906–16. [PubMed: 22780096]
- Fano S, Çalı kan G, Heinemann U. Differential effects of blockade of ERG channels on gamma oscillations and excitability in rat hippocampal slices. *Eur J Neurosci*. 2012; 36(12):3628–35. [PubMed: 23050739]

9. Keefe RS, Harvey PD. Cognitive impairment in schizophrenia. *Handb Exp Pharmacol*. 2012; (213): 11–37. [PubMed: 23027411]
10. Green MF, Kern RS, Braff DL, Mintz J. Neurocognitive deficits and functional outcome in schizophrenia: are we measuring the “right stuff”? *Schizophr Bull*. 2000; 26(1):119–36. [PubMed: 10755673]
11. Mowry BJ, Gratten J. The emerging spectrum of allelic variation in schizophrenia: current evidence and strategies for the identification and functional characterization of common and rare variants. *Mol Psychiatry*. 2013; 18(1):38–52. [PubMed: 22547114]
12. Svrakic DM, Zorumski CF, Svrakic NM, Zwir I, Cloninger CR. Risk architecture of schizophrenia: the role of epigenetics. *Curr Opin Psychiatry*. 2013; 26(2):188–95. [PubMed: 23318661]
13. Apud JA, Zhang F, Decot H, Bigos KL, Weinberger DR. Genetic variation in *KCNH2* associated with expression in the brain of a unique hERG isoform modulates treatment response in patients with schizophrenia. *Am J Psychiatry*. 2012; 169(7):725–34. [PubMed: 22706279]
14. Barker GR, Bird F, Alexander V, Warburton EC. Recognition memory for objects, place, and temporal order: a disconnection analysis of the role of the medial prefrontal cortex and perirhinal cortex. *J Neurosci*. 2007; 27(11):2948–57. [PubMed: 17360918]
15. Papaleo F, Crawley JN, Song J, Lipska BK, Pickel J, Weinberger DR, et al. Genetic dissection of the role of catechol-O-methyltransferase in cognition and stress reactivity in mice. *J Neurosci*. 2008; 28(35):8709–23. [PubMed: 18753372]
16. Barker GR, Warburton EC. When is the hippocampus involved in recognition memory? *J Neurosci*. 2011; 31(29):10721–31. [PubMed: 21775615]
17. Shepard PD, Canavier CC, Levitan ES. Ether-a-go-go-related gene potassium channels: what's all the buzz about? *Schizophr Bull*. 2007; 33(6):1263–9. [PubMed: 17905786]
18. Aultman JM, Moghaddam B. Distinct contributions of glutamate and dopamine receptors to temporal aspects of rodent working memory using a clinically relevant task. *Psychopharmacology (Berl)*. 2001; 153(3):353–64. [PubMed: 11271408]
19. Kellendonk C, Simpson EH, Polan HJ, Malleret G, Vronskaya S, Winiger V, et al. Transient and selective overexpression of dopamine D2 receptors in the striatum causes persistent abnormalities in prefrontal cortex functioning. *Neuron*. 2006; 49(4):603–15. [PubMed: 16476668]
20. Papaleo F, Yang F, Garcia S, Chen J, Lu B, Crawley JN, et al. Dysbindin-1 modulates prefrontal cortical activity and schizophrenia-like behaviors via dopamine/D2 pathways. *Mol Psychiatry*. 2012; 17(1):85–98. [PubMed: 20956979]
21. Weinberger DR. Implications of normal brain development for the pathogenesis of schizophrenia. *Arch Gen Psychiatry*. 1987; 44(7):660–9. [PubMed: 3606332]
22. Pratt J, Winchester C, Dawson N, Morris B. Advancing schizophrenia drug discovery: optimizing rodent models to bridge the translational gap. *Nat Rev Drug Discov*. 2012; 11(7):560–79. [PubMed: 22722532]
23. Shepherd AM, Laurens KR, Matheson SL, Carr VJ, Green MJ. Systematic meta-review and quality assessment of the structural brain alterations in schizophrenia. *Neurosci Biobehav Rev*. 2012; 36(4):1342–56. [PubMed: 22244985]
24. Adriano F, Caltagirone C, Spalletta G. Hippocampal volume reduction in first-episode and chronic schizophrenia: a review and meta-analysis. *Neuroscientist*. 2012; 18(2):180–200. [PubMed: 21531988]
25. Bogerts B, Meertz E, Schönfeldt-Bausch R. Basal ganglia and limbic system pathology in schizophrenia. A morphometric study of brain volume and shrinkage. *Arch Gen Psychiatry*. 1985; 42(8):784–91. [PubMed: 4015323]
26. Zierhut KC, Graßmann R, Kaufmann J, Steiner J, Bogerts B, Schiltz K. Hippocampal CA1 deformity is related to symptom severity and antipsychotic dosage in schizophrenia. *Brain*. 2013; 136(Pt 3):804–14. [PubMed: 23388407]
27. Goldman AL, Pezawas L, Mattay VS, Fischl B, Verchinski BA, Zolnick B, et al. Heritability of brain morphology related to schizophrenia: a large-scale automated magnetic resonance imaging segmentation study. *Biol Psychiatry*. 2008; 63(5):475–83. [PubMed: 17727823]

28. Owens SF, Picchioni MM, Rijdsdijk FV, Stahl D, Vassos E, Rodger AK, et al. Genetic overlap between episodic memory deficits and schizophrenia: results from the Maudsley Twin Study. *Psychol Med.* 2011; 41(3):521–32. [PubMed: 20459888]
29. Hanlon FM, Weisend MP, Hamilton DA, Jones AP, Thoma RJ, Huang M, et al. Impairment on the hippocampal-dependent virtual Morris water task in schizophrenia. *Schizophr Res.* 2006; 87(1–3): 67–80. [PubMed: 16844347]
30. Diano S, Farr SA, Benoit SC, McNay EC, da Silva I, Horvath B, et al. Ghrelin controls hippocampal spine synapse density and memory performance. *Nat Neurosci.* 2006; 9(3):381–8. [PubMed: 16491079]
31. Mumby DG, Pinel JP. Rhinal cortex lesions and object recognition in rats. *Behav Neurosci.* 1994; 108(1):11–8. [PubMed: 8192836]
32. Ennaceur A, Neave N, Aggleton JP. Neurotoxic lesions of the perirhinal cortex do not mimic the behavioural effects of fornix transection in the rat. *Behav Brain Res.* 1996; 80(1–2):9–25. [PubMed: 8905124]
33. Asrar S, Kaneko K, Takao K, Negandhi J, Matsui M, Shibasaki K, et al. DIP/WISH deficiency enhances synaptic function and performance in the Barnes maze. *Mol Brain.* 2011; 4:39. [PubMed: 22018352]
34. Huerta PT, Sun LD, Wilson MA, Tonegawa S. Formation of temporal memory requires NMDA receptors within CA1 pyramidal neurons. *Neuron.* 2000; 25(2):473–80. [PubMed: 10719900]
35. Skucas VA, Mathews IB, Yang J, Cheng Q, Treister A, Duffy AM, et al. Impairment of select forms of spatial memory and neurotrophin-dependent synaptic plasticity by deletion of glial aquaporin-4. *J Neurosci.* 2011; 31(17):6392–7. [PubMed: 21525279]
36. Lipska BK, Weinberger DR. To model a psychiatric disorder in animals: schizophrenia as a reality test. *Neuropsychopharmacology.* 2000; 23(3):223–39. [PubMed: 10942847]
37. Lee H, Dvorak D, Kao HY, Duffy Á, Scharfman HE, Fenton AA. Early cognitive experience prevents adult deficits in a neurodevelopmental schizophrenia model. *Neuron.* 2012; 75(4):714–24. [PubMed: 22920261]
38. Lodge DJ, Grace AA. Gestational methylazoxymethanol acetate administration: a developmental disruption model of schizophrenia. *Behav Brain Res.* 2009; 204(2):306–12. [PubMed: 19716984]
39. Pocivavsek A, Wu HQ, Elmer GI, Bruno JP, Schwarcz R. Pre- and postnatal exposure to kynurenine causes cognitive deficits in adulthood. *Eur J Neurosci.* 2012; 35(10):1605–12. [PubMed: 22515201]
40. Weinberger DR, Egan MF, Bertolino A, Callicott JH, Mattay VS, Lipska BK, et al. Prefrontal neurons and the genetics of schizophrenia. *Biol Psychiatry.* 2001; 50(11):825–44. [PubMed: 11743939]
41. Wang M, Gamo NJ, Yang Y, Jin LE, Wang XJ, Laubach M, et al. Neuronal basis of age-related working memory decline. *Nature.* 2011; 476(7359):210–3. [PubMed: 21796118]
42. Artchakov D, Tikhonravov D, Ma Y, Neuvonen T, Linnankoski I, Carlson S. Distracters impair and create working memory-related neuronal activity in the prefrontal cortex. *Cereb Cortex.* 2009; 19(11):2680–9. [PubMed: 19329569]
43. Wen L, Lu YS, Zhu XH, Li XM, Woo RS, Chen YJ, et al. Neuregulin 1 regulates pyramidal neuron activity via ErbB4 in parvalbumin-positive interneurons. *Proc Natl Acad Sci U S A.* 2010; 107(3): 1211–6. [PubMed: 20080551]
44. Heide J, Mann SA, Vandenberg JI. The schizophrenia-associated Kv11.1-3.1 isoform results in reduced current accumulation during repetitive brief depolarizations. *PLOS One.* 2012; 7(9)
45. Cardoso-Cruz H, Lima D, Galhardo V. Impaired spatial memory performance in a rat model of neuropathic pain is associated with reduced hippocampus-prefrontal cortex connectivity. *J Neurosci.* 2013; 33(6):2465–80. [PubMed: 23392675]
46. Howard MW, Rizzuto DS, Caplan JB, Madsen JR, Lisman J, Aschenbrenner-Scheibe R, et al. Gamma oscillations correlate with working memory load in humans. *Cereb Cortex.* 2003; 13(12): 1369–74. [PubMed: 14615302]
47. Tallon-Baudry C, Bertrand O, Peronnet F, Pernier J. Induced gamma-band activity during the delay of a visual short-term memory task in humans. *J Neurosci.* 1998; 18(11):4244–54. [PubMed: 9592102]

48. Papaleo F, Lipska BK, Weinberger DR. Mouse models of genetic effects on cognition: relevance to schizophrenia. *Neuropharmacology*. 2012; 62(3):1204–20. [PubMed: 21557953]
49. Owen MJ. Implications of genetic findings for understanding schizophrenia. *Schizophr Bull*. 2012; 38(5):904–7. [PubMed: 22987847]

Author Manuscript

Author Manuscript

Author Manuscript

Author Manuscript

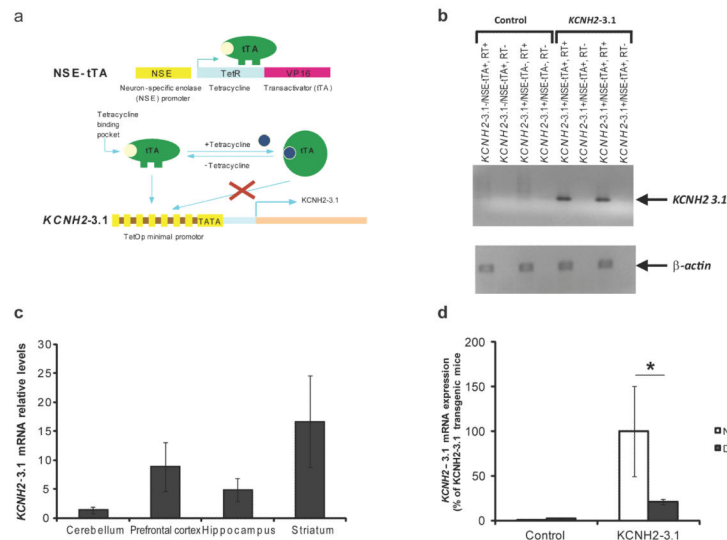


### Figure 1. *KCNH2-3.1* transgene expression

(a) A schematic of the *KCNH2-3.1* transgene construct. The tetracycline transactivator (tTA) is under the control of the neuron-specific enolase (NSE) promoter. The *KCNH2-3.1* gene is under the control of the tetracycline-responsive promoter, TetOp. Administration of a tetracycline antibiotic turns off expression of the *KCNH2-3.1* gene. (b) qRT-PCR data for *KCNH2-3.1* mRNA taken from the prefrontal cortex. The four lanes on the left (control) are samples from mice that did not have both transgenes and thus were not expected to express *KCNH2-3.1* mRNA. These lanes confirm that there is no endogenous expression of *KCNH2-3.1* mRNA in mice and no “leaky” expression of *KCNH2-3.1* mRNA without the NSE-tTA promoter. The four lanes on the right (*KCNH2-3.1*) are samples from mice that had both transgenes and would be expected to express *KCNH2-3.1* mRNA. The first and third lanes show the expected bands corresponding to *KCNH2-3.1* mRNA. The second and fourth lanes in this group do not have this band because of the absence of reverse transcriptase (RT<sup>-</sup>) meaning there was no genomic DNA contamination in the RNA samples. (c) Relative expression of *KCNH2-3.1* mRNA in specific regions of the brain of *KCNH2-3.1* transgenic mice measured by qRT-PCR. N = 5. Values are normalized to expression levels in the cerebellum. (d) *KCNH2-3.1* expression in the PFC in mice treated with doxycycline. Doxycycline treatment significantly reduced the expression of *KCNH2-3.1* in *KCNH2-3.1* transgenic mice [ $t(10) = 1.88, p = 0.04$ ]. n = 5/non-treated control; n = 5/non-treated *KCNH2-3.1* transgenic; n = 3/treated control; n = 7/treated *KCNH2-3.1* transgenic. \* $p < 0.05$ . In panels c and d, data are represented as the mean  $\pm$  SEM.

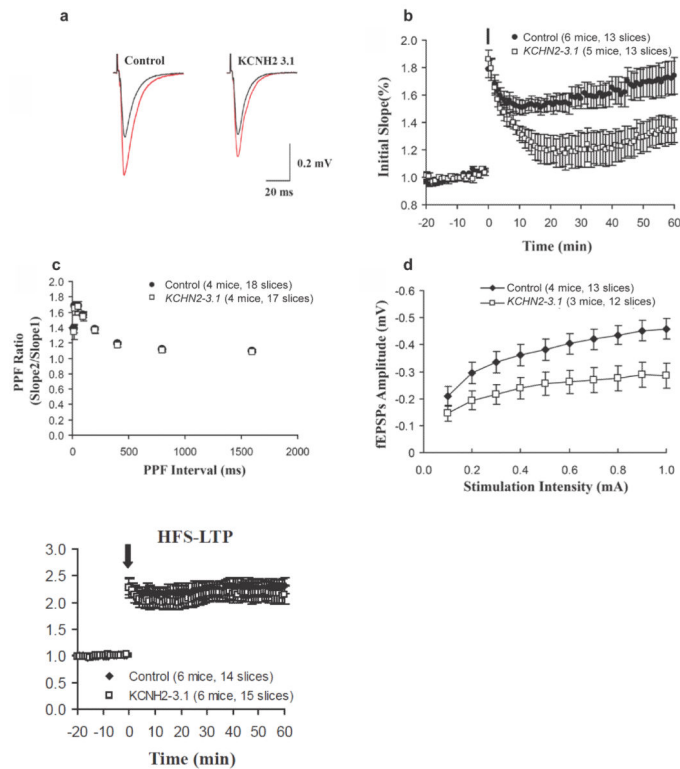


### Figure 2. Impaired TBS-LTP in *KCNH2-3.1* transgenic mice

Slices from *KCNH2-3.1* transgenic mice display impaired LTP. LTP was induced by TBS. (a) Example fEPSP recordings before (black lines) and 60 min after LTP induction (red lines). (b) Complete time courses are shown for the complete samples. TBS only induced a  $133 \pm 10\%$  potentiation in *KCNH2-3.1* mice, whereas it induced a  $171 \pm 11\%$  potentiation in *KCNH2-3.1* mice ( $p = 0.015$ , t-test).  $n = 6$ /control mice and  $n = 5$ /*KCNH2-3.1*. (c) Normal paired pulse facilitation (PPF) in young and adult *KCNH2-3.1* mice. The ratios of the second and first EPSP slopes were calculated, and mean values are plotted against different inter-pulse intervals (IPI, 12.5 to 1600 msec).  $n = 4$ /control mice and  $n = 4$ /*KCNH2-3.1*. (d) Impaired basal synaptic transmission in adult *KCNH2-3.1* mice. Input-output curves were generated by plotting the postsynaptic response (initial slope of fEPSP) as a function of the stimulation intensity.  $n = 4$ /control mice and  $n = 3$ /*KCNH2-3.1*. (e) In contrast to, TBS-LTP, HFS-LTP is normal in *KCNH2-3.1* mice.  $n = 6$ /control mice and  $n = 6$ /*KCNH2-3.1*. Data are represented as the mean  $\pm$  SEM.

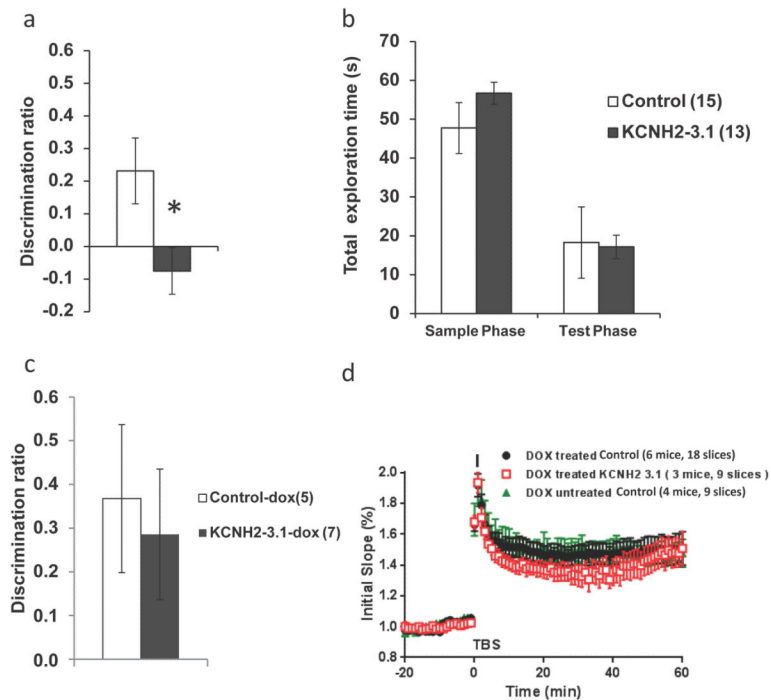


**Figure 3. Effects of *KCNH2* transgene expression on object location performance**

(a) Performance of control and *KCNH2-3.1* transgenic mice in the object location task. Control mice demonstrated a significant preference for exploration of the displaced object [ $t(14) = 2.29, p = 0.038$ ]. The control mice were significantly different from *KCNH2-3.1* transgenic mice [ $t(26) = 2.41, p = 0.023$ ], which showed no preference [ $t(12) = 1.06, p = 0.306$ ] for the displaced object. The discrimination ratio represented the time spent exploring the displaced object minus time spent exploring the object in the familiar location divided by the total exploration time. (b) There were no genotype differences in total exploration in either the sample [ $t(26) = 0.81, p = 0.425$ ] or test phase [ $t(26) = 0.27, p = 0.789$ ].  $n = 15$ /control and  $n = 13$ /*KCNH2-3.1* in panels a and b. (c) Treatment with doxycycline (200  $\mu\text{g}/\text{mL}$ ) in the drinking water reversed the object location deficit in *KCNH2-3.1* transgenic mice giving them a discrimination ratio not significantly different from control mice [ $t(10) = 0.36, p = 0.73$ ].  $n = 5$ /control and  $n = 7$ /*KCNH2-3.1* (d) TBS-LTP is comparable between dox-treated *KCNH2-3.1* transgenic, dox-treated control, and untreated control mice ( $147 \pm 9\%$ ,  $151 \pm 10\%$ ,  $147 \pm 6\%$  at 50–60 min, respectively). Data are represented as the mean  $\pm$  SEM.

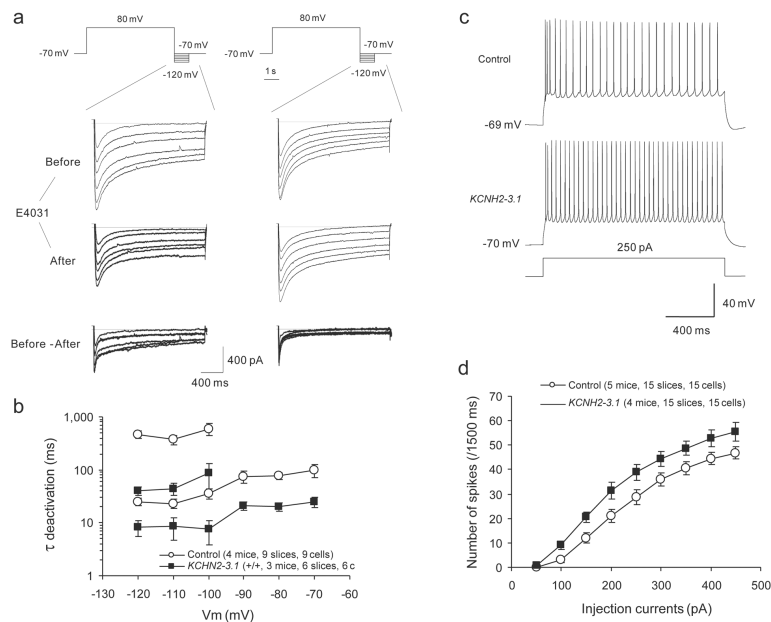


#### Figure 4. Increased firing rate in PFC pyramidal neurons

(a) Representative KCNH2-mediated tail currents in control and *KCNH2-3.1* transgenic mice neurons in cortical slices before and after application of E4031. Top plot diagrams the voltage protocol. Tail currents evoked by voltage pulses (1 s) to potentials between  $-120$  mV and  $-70$  mV in 10-mV increments, following steps (6 s) to 80 mV. Traces represent tail currents of pyramidal neurons in both control and *KCNH2-3.1* mice, respectively. Bottom plot represents E-4031-sensitive current generated by subtracting the before inhibitor and after inhibitor currents. (b) Semilogarithmic plot of deactivation time constants of neurons in slice. The bottom plots are for  $\tau_1$  and the top plots are for  $\tau_2$ . There was a significant increase in  $\tau_1$  [ $F(5, 65) = 5.29, p < 0.001$ ] as the repolarizing voltage increased. Neurons from *KCNH2-3.1* transgenic mice had significantly lower  $\tau_1$  [ $F(1, 13) = 23.97, p < 0.001$ ] and  $\tau_2$  [ $F(1, 13) = 32.09, p < 0.001$ ] values across repolarizing voltages.  $n = 4/\text{control}$  and  $n = 3/\text{KCNH2-3.1}$ . (c) Representative trace showing the higher firing rate of a neuron from a *KCNH2-3.1* transgenic mouse (bottom trace) compared to a control mouse (top trace) during injection of 250 pA current. (d) mPFC neurons from *KCNH2-3.1* transgenic mice produced more action potentials in response to current injections. Both genotypes showed increased firing rates in response to increased current injections [ $F(8, 224) = 218.31, p < 0.001$ ]. Neurons from *KCNH2-3.1* transgenic mice had significantly higher firing rates across all stimulation levels [ $F(1, 28) = 8.65, p = 0.006$ ] without a specific genotype X current amplitude interaction [ $F(8, 224) = 1.32, p < 0.234$ ].  $n = 5/\text{control}$  and  $n = 4/\text{KCNH2-3.1}$ . Data are represented as the mean  $\pm$  SEM.

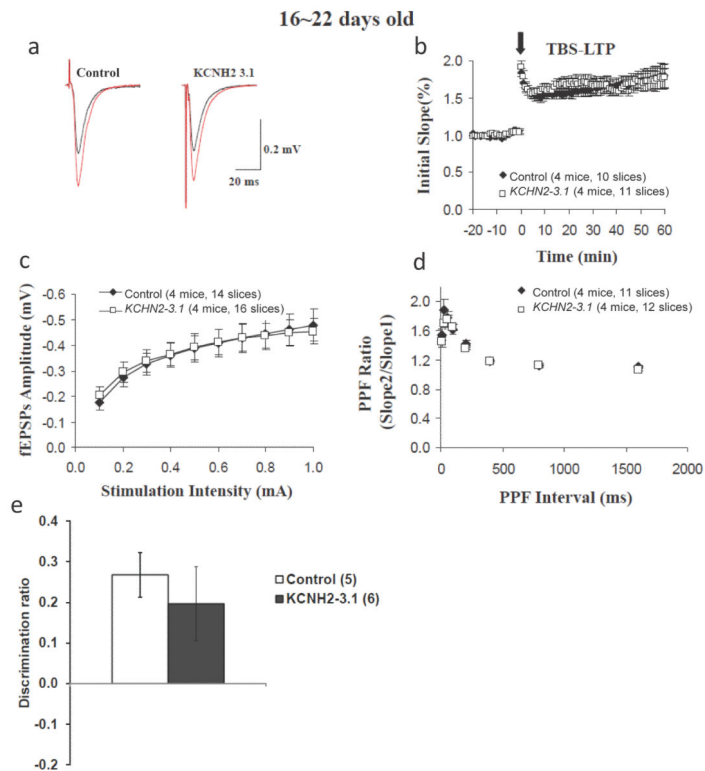


**Figure 5. Effects of *KCNH2-3.1* transgene expression on hippocampal function and behavior in juvenile mice**

(a–b) *KCNH2-3.1* transgenic mice display normal TBS-LTP. TBS-LTP was induced by 4 TBS at 100 Hz (black arrow in B) in 16–22 days old animals (*KCNH2-3.1* transgenic mice and control littermates). Example fEPSP recordings before (black lines) and 60 min after TBS-LTP induction (red lines) are shown in a and the complete time courses are shown in b. TBS-LTP is comparable between *KCNH2-3.1* transgenic mice and control mice ( $176 \pm 15\%$  vs.  $173 \pm 13\%$  at 50–60 min, respectively). (c) Normal basal synaptic transmission in young *KCNH2-3.1* mice. Input-output curves were generated by plotting the postsynaptic response (initial slope of fEPSP) as a function of the stimulation intensity. (d) Normal paired pulse facilitation (PPF) in young mice. The ratios of the second and first EPSP slopes were calculated, and mean values are plotted against different inter-pulse intervals (IPI, 12.5 to 1600 msec). (e) In contrast to adults, juvenile *KCNH2-3.1* transgenic mice show no difference in object location memory compared to control littermates [ $t(10) = 0.67$ ,  $p = 0.519$ ]. Data are represented as mean  $\pm$  SEM.